Supplementary information

to the article "Cationic and anionic phenothiazine derivatives: electrochemical behavior and application in DNA-sensor development" of Anastasia N. Malanina, Yury I. Kuzin, Pavel L. Padnya, Alexey N. Ivanov, Ivan I. Stoikov and Gennady A. Evtugyn

Synthesis of phenothiazine derivatives PhTz-$(NH_2)_2$ and PhTz-$(COOH)_2$.

The ^{1}H NMR spectra were recorded on a Bruker Avance 400 spectrometer (400 MHz) for 3-5% solutions in DMSO-d_6. The residual solvent peaks were used as an internal standard. Elemental analysis was performed on Perkin–Elmer 2400 Series II instruments. Most chemicals were purchased from Aldrich and used as received without additional purification. Organic solvents were purified in accordance with standard procedures.

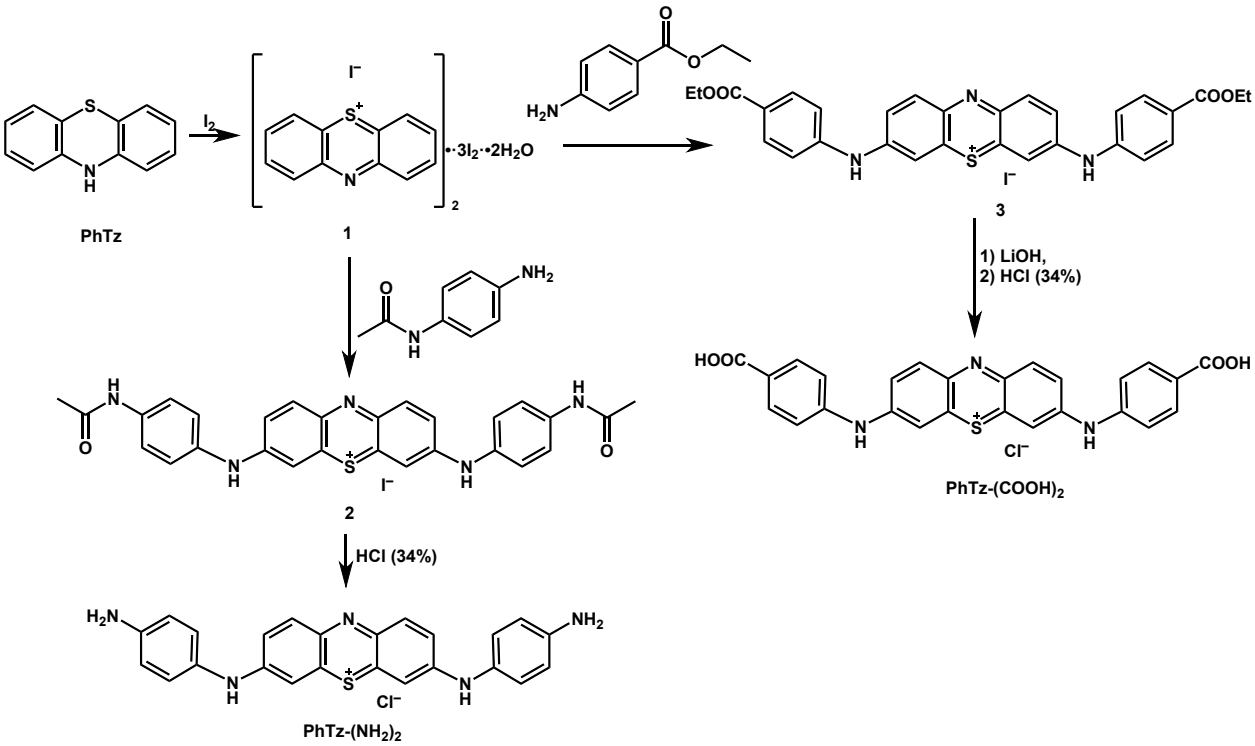

Scheme S1. Synthesis of PhTz-$(NH_2)_2$ and PhTz-$(COOH)_2$.

3,7-bis((4-aminophenyl)amino)phenothiazin-5-ium chloride (PhTz-$(NH_2)_2$).

A solution of *p*-aminoacetanilide (0.579 g, 3.86 mmol) in methanol (20 mL) was added to a suspension of phenothiazin-5-ium tetraiodide (compound 1) (0.300 g, 0.425 mmol). Mixture was vigorously stirred at room temperature for 24 h. The obtained intensively colored solution was filtered. Precipitate of compound 2 was washed with methanol. Then, the resulting compound 2 was dissolved in the mixture of propan-2-ol (20 mL) and concentrated hydrochloric acid (20 mL) and was refluxed for 120 h. The solvent was evaporated. The precipitate formed was filtered off and washed with 2 M HCl.

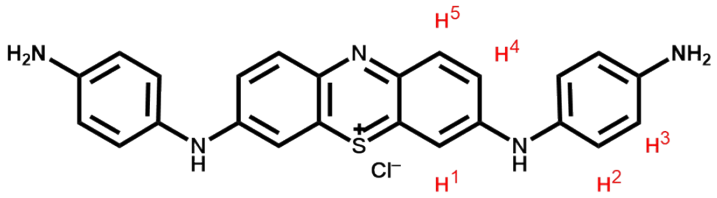

^{1}H NMR (DMSO-d_6, 298 K, 400 MHz), δ_H: 8.34 (s, 2H, NH), 7.61 (d, J = 8.0 Hz, 2H, H(4)), 6.91 (m, 4H, H(5), H(1)), 6.50 (m, 8H, H(3), H(2)), 5.20 (s, NH_2). Elem. Anal. Calcd. for $C_{24}H_{20}ClN_5S$ (%): C, 64.64; H, 4.52; Cl, 7.95; N, 15.70; S, 7.19. Found (%):C, 64.68; H, 4.47; Cl, 7.91; N, 15.73; S, 7.21.

3,7-bis((4-carboxyphenyl)amino)phenothiazin-5-ium chloride (PhTz-$(COOH)_2$).

A solution of benzocaine (0.637 g, 3.86 mmol) in methanol (20 mL) was added to a suspension of phenothiazin-5-ium tetraiodide (compound 1) (0.300 g, 0.425 mmol). The mixture was vigorously stirred at room temperature for 24 h. The obtained intensively colored solution was filtered. The precipitate of compound 3 was washed with methanol. Then, lithium hydroxide monohydrate (tenfold excess by moles) and THF (20 mL) were added to the resulting compound 3, and water (2 mL) was added with vigorous stirring. The mixture was refluxed for 8 h. The solvent was evaporated on a rotary evaporator, and then concentrated hydrochloric acid was added to the residue. The obtained mixture was vigorously stirred at room temperature for 10 h. The precipitate formed was filtered off and washed with 2 M HCl.

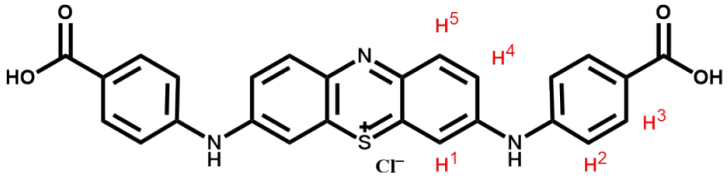

^{1}H NMR (DMSO-d_6, 298 K, 400 MHz), δ_H: 11.60 (s, 2H, NH), 8.22 (d, J = 9.3 Hz, 2H, H(4)), 8.07 (d, J = 8.3 Hz, 4H, H(3)), 7.91 (s, 2H, H(1)), 7.76 (d, J = 9.4 Hz, 2H, H(5)), 7.61 (d, J = 8.2 Hz, 4H, H(2)). Elem. Anal. Calcd. for $C_{26}H_{18}ClN_3O_4S$ (%): C, 61.97; H, 3.60; Cl, 7.03; N, 8.34; S, 6.36. Found (%): C, 61.94; H, 3.63; Cl, 7.07; N, 8.38; S, 6.32.

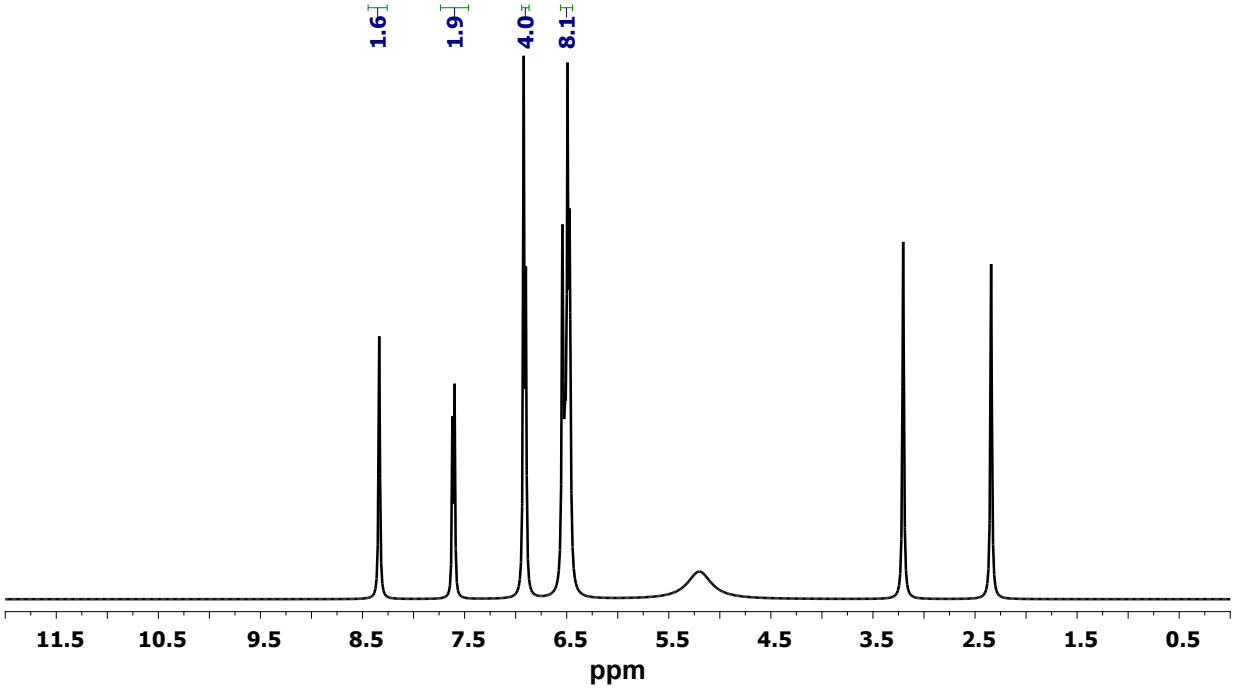

Figure S1. ^{1}H NMR spectrum of PhTz-$(NH_2)_2$ (DMSO-d_6, 298 K, 400 MHz).

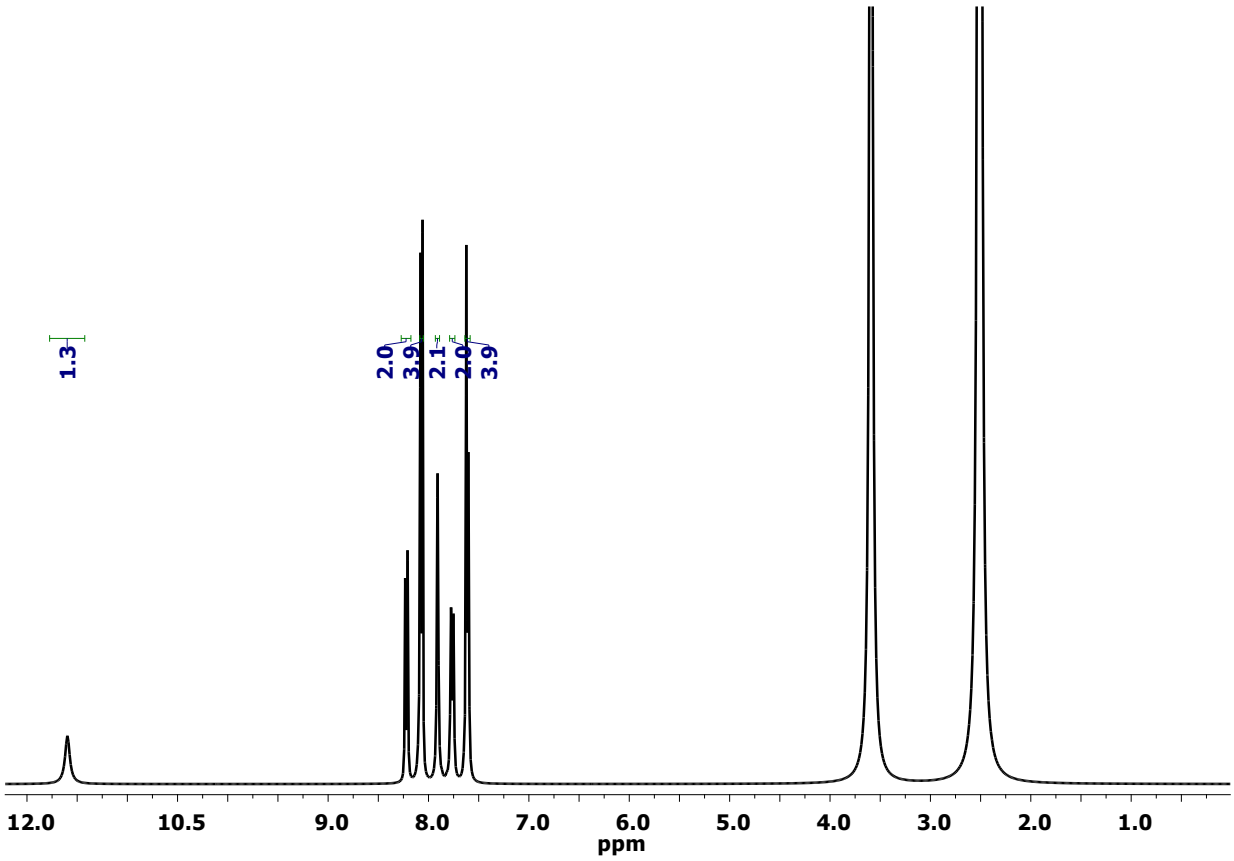

Figure S2. ^{1}H NMR spectrum of PhTz-$(COOH)_2$ (DMSO-d_6, 298 K, 400 MHz).

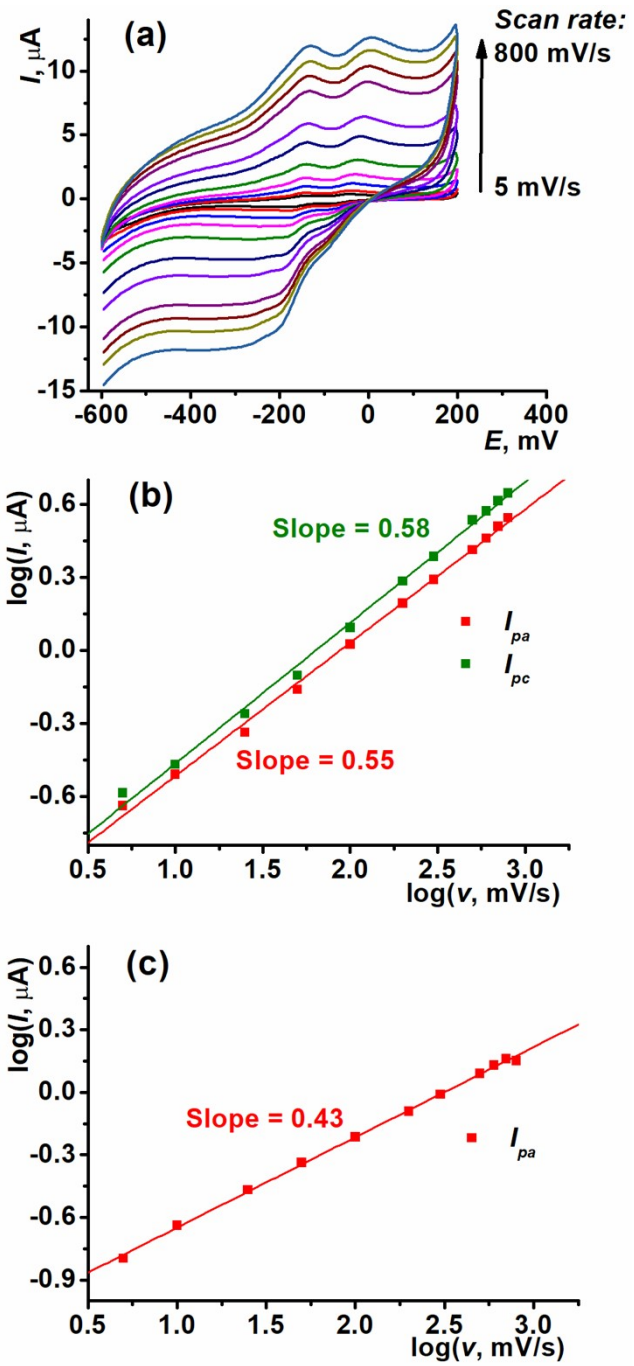

Figure S3. Cyclic voltammograms of the mixture of 100 μM PhTz-$(NH_2)_2$ and 100 μM PhTz-$(COOH)_2$ recorded with various potential scan rates (a); bi-logarithmic dependencies of the peak currents on the scan rate for PhTz-$(NH_2)_2$ (b); bi-logarithmic dependencies of the anodic peak current on the scan rate for PhTz-$(COOH)_2$ (c).

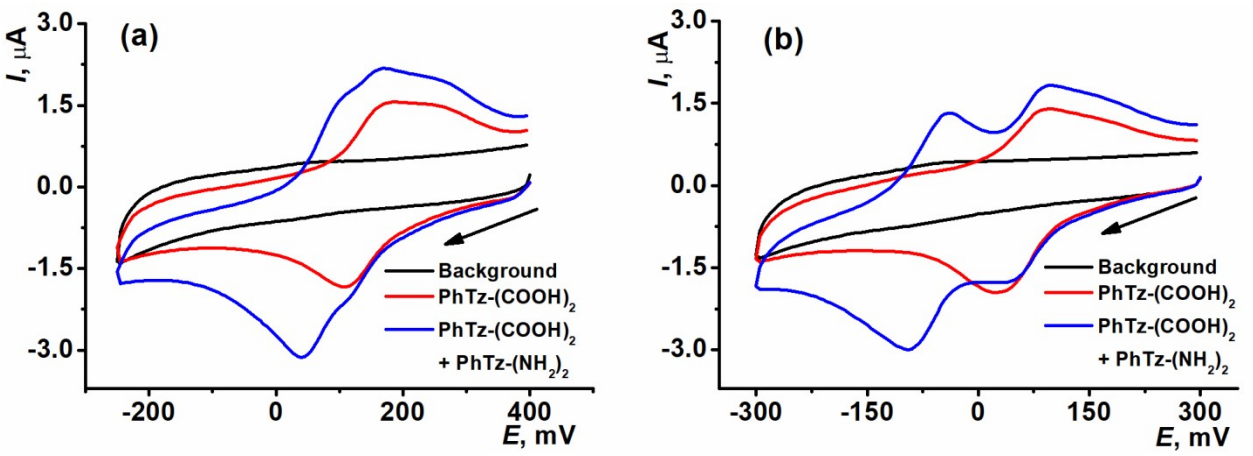

Figure S4. Cyclic voltammograms of 100 μM PhTz-$(NH_2)_2$ and 100 μM PhTz-$(COOH)_2$ at pH 2.5 (a) and 4.0 (b). BR buffer – acetonitrile (1:1 vol.), scan rate 100 mV/s.

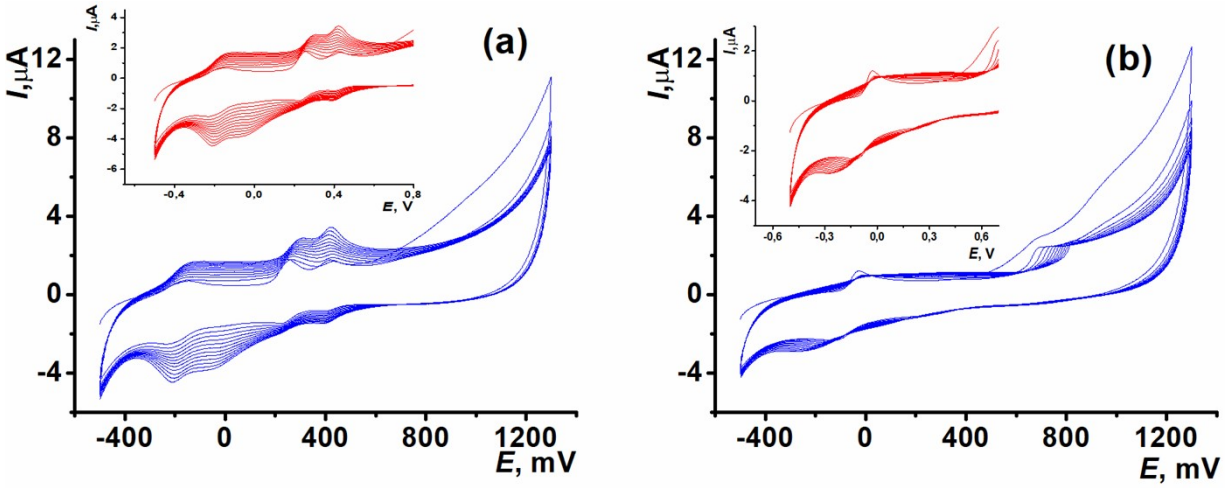

Figure S5. Cycling voltammograms of 100 μM PhTz-$(NH_2)_2$ (a) and 100 μM PhTz-$(COOH)_2$ (b) recorded on GCE in BR buffer mixed with acetonitrile (1:1 vol.), pH = 7.0. Scan rate 100 mV/s, 12 cycles. Insets – potential area corresponded to the phenothiazine core redox reactions.

Table S1 The EIS parameters obtained for GCE covered with polymeric films obtained from 100 μM PhTz-$(COOH)_2$ (1), 100 μM PhTz-$(NH_2)_2$ (2), their mixture (3), that after deposition of DNA (4), for films obtained after consecutive electropolymerization of 100 μM PhTz-$(COOH)_2$ and 100 μM PhTz-$(NH_2)_2$ (5), that after deposition of DNA (6). Electrode – polymer interface, R_s – solution resistance, R_{ct} – charge transfer resistance, CPE – constant phase element, N – exponential factor.

No	R_s, Ω	R_{ct}, kΩ	CPE, μMho	N
1	100.3 ± 1.2	5.9 ± 0.3	10.1 ± 1.1	0.822 ± 0.019
2	113.3 ± 4.2	65.0 ± 1.2	21.4 ± 0.6	0.765 ± 0.014
3	117.9 ± 3.6	281.0 ± 8.2	21.5 ± 1.2	0.767 ± 0.016
4	112.7 ± 4.0	310.7 ± 6.8	11.92 ± 0.7	0.773 ± 0.011
5	111.6 ± 4.8	316.7 ± 7.8	56.7 ± 1.4	0.861 ± 0.018
6	116.1 ± 3.5	427.2 ± 6.9	48.6 ± 1.3	0.876 ± 0.018

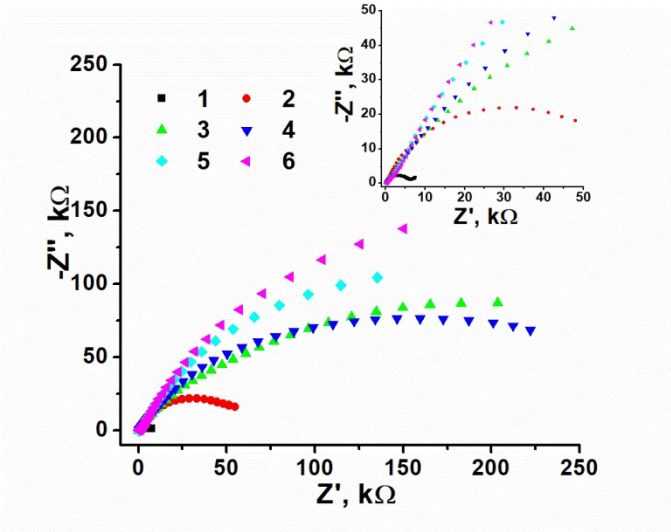

Figure S6. The Nyquist diagrams recorded on the GCE covered with the polymeric film obtained from 100 μM PhTz-$(COOH)_2$ (1), 100 μM PhTz-$(NH_2)_2$ (2), their mixture (3) and that after deposition of DNA (4); for films obtained after consecutive electropolymerization of 100 μM PhTz-$(COOH)_2$ and 100 μM PhTz-$(NH_2)_2$ (5) and that after deposition of DNA (6)

Generalized Additive Mixed Models (GAMMs) for modeling redox-peak current dependencies on phenothiazine concentrations

The concentrations of PhTz-$(COOH)_2$ and PhTz-$(NH_2)_2$, referred to as **CPhTz1** and **CPhTz2**, respectively, were evaluated using a full factorial experimental design. Concentration levels of **CPhTz1** and **CPhTz2** were set at 0, 25, 50, 100, 150, and 200 μM, with each combination measured 3 to 9 times. GAMMs were employed to analyze their effects on anodic ($\mathbf{Ip_a}$) and cathodic ($\mathbf{Ip_c}$) peak currents of electrodeposited materials.

A preliminary analysis confirmed that the residuals of the measured data followed a normal distribution, which is appropriate for regression modeling. The probability density function $f_Y(\mu,\sigma^2)$ of the random variable Y, representing peak currents, is defined as (1):

$$f_Y(\mu,\sigma^2) = \frac{1}{\sqrt{2\pi\sigma^2}} e^{-\frac{1(\cdot}{2}} \quad (1)$$

where μ is the mean value of the modeled parameter (peak current) and σ is the standard deviation of residuals.

The linear predictor μ, which models the relationship between phenothiazine concentrations and peak currents, is described as (2):

$$\mu = a_0 + ti(CPhTz1) + ti(CPhTz2) + ti(CPhTz1,CPhTz2) \quad (2)$$

Here, a_0 is an intercept term, ti represents smooth tensor product interaction terms based on thin-plate regression splines with extra shrinkage. Thus, $ti(CPhTz1)$ and $ti(CPhTz2)$ are univariate smooth terms representing the individual effects of **CPhTz1** and **CPhTz2.** $ti(CPhTz1,CPhTz2)$ is a bivariate smooth term accounting for the interaction between **CPhTz1** and **CPhTz2**. This model structure allows for a detailed exploration of main effects and interactions, particularly where the influence of one parameter depends on the value of the other. The same model structure was applied to analyze all dependencies of $\mathbf{Ip_a}$ and $\mathbf{Ip_c}$.

Smooth terms in GAMMs are essential for capturing nonlinear relationships between dependent and independent variables. These terms provide flexibility by allowing the degree of smoothness to vary across different covariates. Smooth tensor product interaction terms, in particular, enable nuanced modeling of interactions by allowing each covariate to have a distinct degree of smoothness. The smoothness of these terms is estimated during the model-fitting process, ensuring an optimal balance between underfitting and overfitting. Additionally, these

terms are invariant to linear rescaling of covariates, meaning they remain consistent and interpretable regardless of the units or scales of the measured variables.

Conventional regression models often assume constant residual dispersion. However, in this analysis, residual dispersion varied with the mean value (μ), indicating heteroscedasticity. To address this issue, the variance parameter (σ^2) was modeled using the following function (3):

$$\sigma^2(\mu) = |\mu|^{2\theta} \quad (3)$$

where $\sigma^2(\mu)$ denotes the variance function evaluated at μ, θ is a power exponent parameter that controls how the variance changes with.

The adequacy of the regression models was evaluated through diagnostic plots, including normalized residuals versus explanatory variables and μ, as well as histograms of residuals and normal Q-Q plots. These visual assessments indicate that the residuals for all models follow an approximately normal distribution, with Q-Q plots showing a close-to-linear relationship. The normality of the residuals was further confirmed using quantitative statistical tests, including the Kolmogorov-Smirnov, Cramér-von Mises, and Anderson-Darling tests. The results of these tests support the adequacy of the regression models, with significance levels exceeding 40%.

The estimated significance of smooth terms and the adjusted R^2 values for the models are presented in Tables S2, S3, and S4. The degree of smoothness for the smooth terms, represented as estimated degrees of freedom (EDF), is automatically selected using generalized cross-validation. This approach optimizes model prediction while minimizing variability in the smooth terms. The adjusted R^2 is a modified version of R^2 that accounts for the number of predictors included in the model. It increases when a new term improves the model's predictive ability more than would be expected by chance and decreases when a term contributes less improvement than anticipated. Adjusted R^2 is a reliable metric for evaluating model performance and understanding how the addition of independent variables impacts the model's explanatory power.

Modelling Ip_a and Ip_c of polymeric films prepared via electropolymerization in mixed solutions of phenothiazines.

Table S2. EDF and Significance (p-value) of smooth terms for models predicting **Ip_a** and **Ip_c** of polymeric films prepared via electropolymerization in mixed solutions of phenothiazines.

Smoothing Term	EDF (p-value)	
	Ip_a	**Ip_c**
ti(CPhTz1)	1.18 (< 0.001)	3.04 (< 0.001)
ti(CPhTz2)	3.52 (< 0.001)	3.27 (< 0.001)

ti(CPhTz1, CPhTz2)	2.98 (0.023)	2.53 (0.049)
Adjusted R^2	0.841	0.713

All smoothing terms were found to be significant for both $\mathbf{Ip_a}$ and $\mathbf{Ip_c}$, although the interaction term showed lower significance, particularly for $\mathbf{Ip_a}$. Plots of the component smooth functions for $\mathbf{Ip_a}$ and $\mathbf{Ip_c}$ are presented in Figures S7 and S8 (panels A, B, C), alongside plots of the model predictions (Figures S7 and S8, panel D).

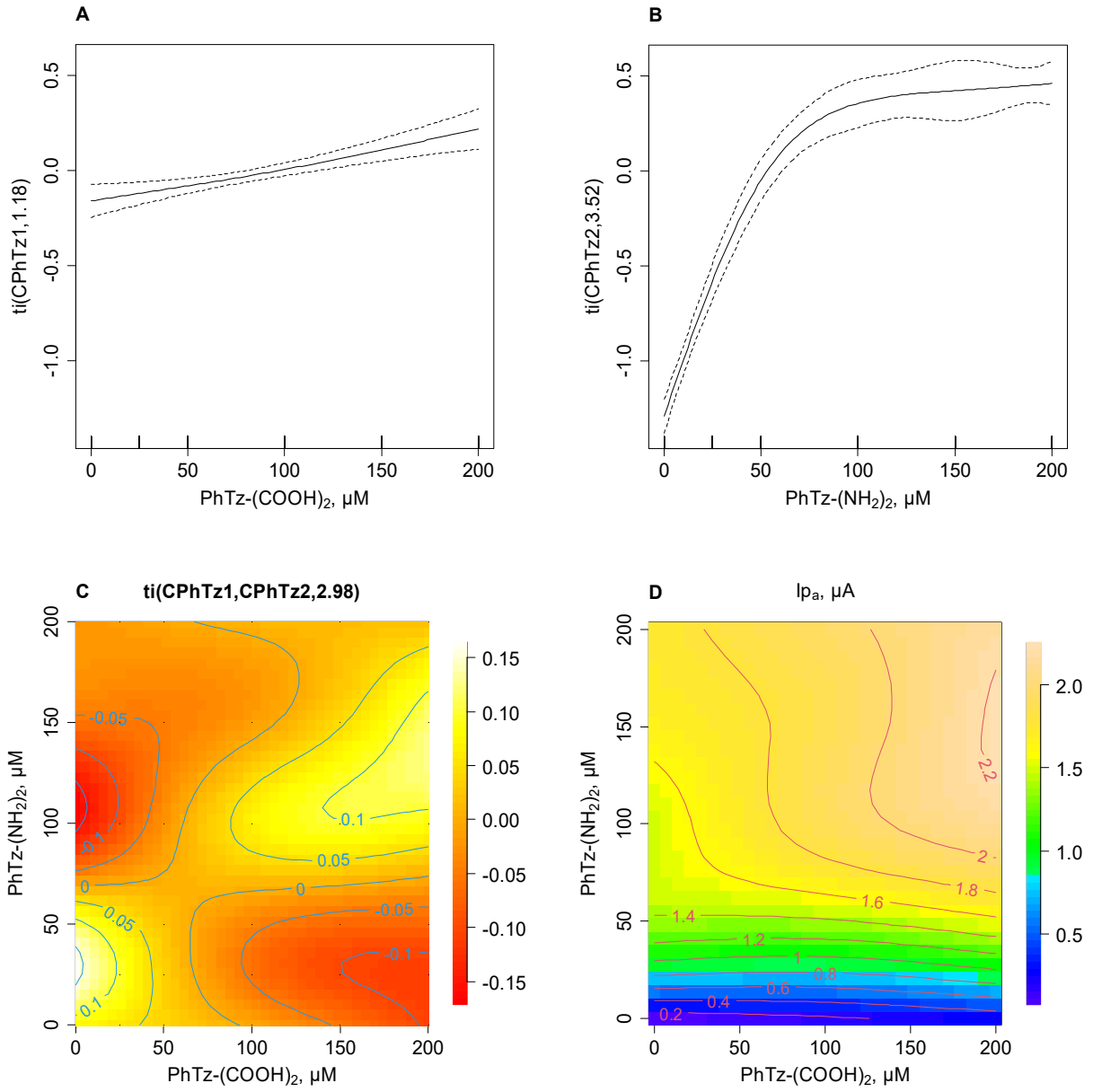

Figure S7. The component smooth functions (A, B, C) and model predictions (D) for $\mathbf{Ip_a}$ of polymeric films prepared via electropolymerization in mixed solutions of phenothiazines. The dashed lines in A and B represent 2 standard errors above and below the estimated smooth function being plotted.

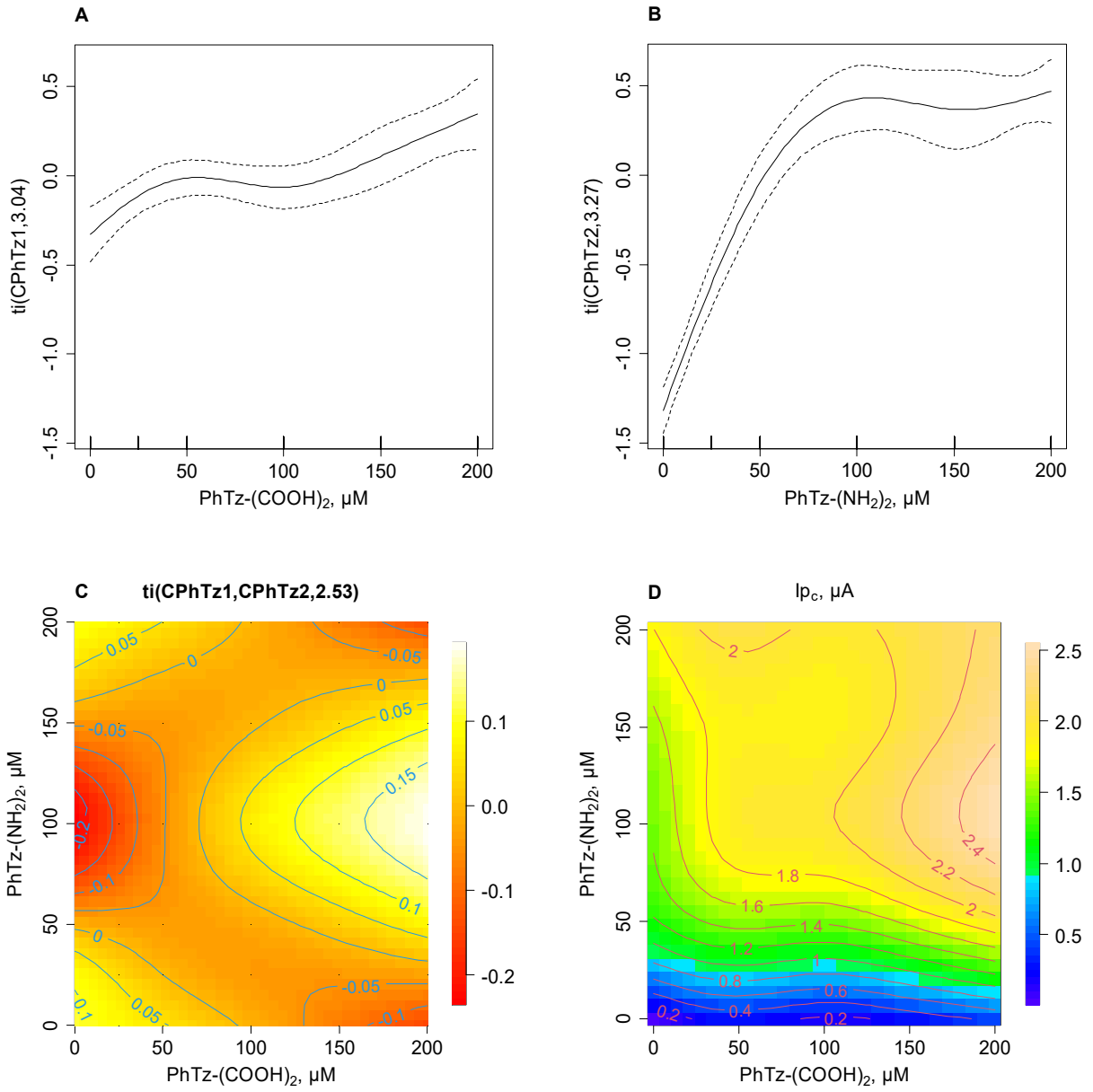

Figure S8. The component smooth functions (A, B, C) and model predictions (D) for $\mathbf{Ip_c}$ of polymeric films prepared via electropolymerization in mixed solutions of phenothiazines. The dashed lines in A and B represent 2 standard errors above and below the estimated smooth function being plotted.

Modelling $\mathbf{Ip_a}$ and $\mathbf{Ip_c}$ of polymeric films prepared through consecutive electropolymerization in individual phenothiazine solutions.

Table S3. EDF and Significance (p-value) of smooth terms for models predicting $\mathbf{Ip_a}$ and $\mathbf{Ip_c}$ of polymeric films prepared through consecutive electropolymerization in individual phenothiazine solutions.

Smoothing Term	EDF (p-value)	
	Ip_a	**Ip_c**
ti(CPhTz1)	0.63 (0.106)	2.73 (< 0.001)
ti(CPhTz2)	3.38 (< 0.001)	3.01 (< 0.001)
ti(CPhTz1, CPhTz2)	8.69 (< 0.001)	4.52 (< 0.001)
Adjusted R^2	0.654	0.647

All smoothing terms were found to be significant for both **Ip_a** and **Ip_c**, except the smoothing term of CPhTz1 for **Ip_a** and therefore it almost shrunk to zero. Plots of the component smooth functions for **Ip_a** and **Ip_c** are presented in Figures S9 and S10 (panels A, B, C), alongside plots of the model predictions (Figures S9 and S10, panel D).

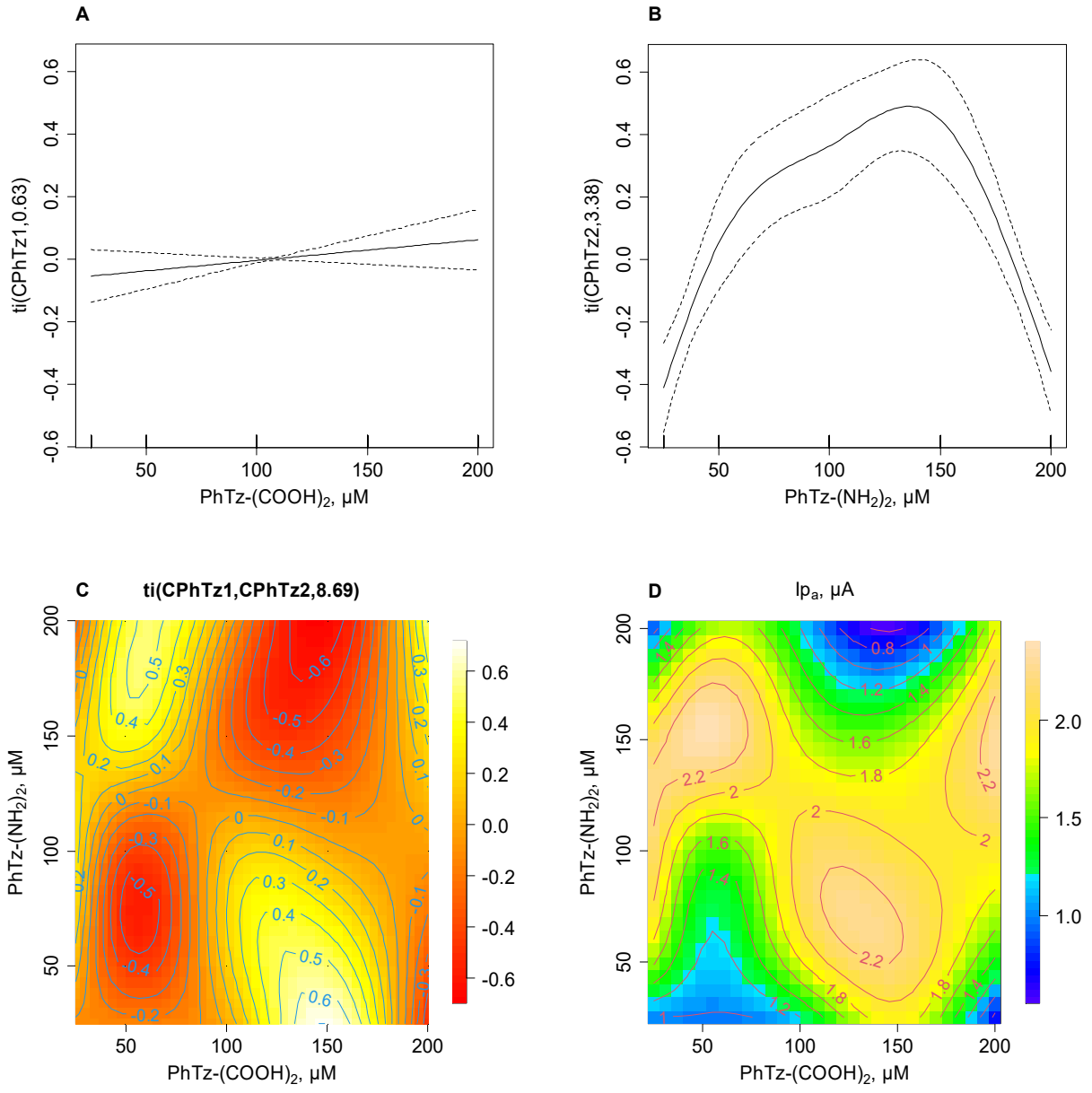

Figure S9. The component smooth functions (A, B, C) and model predictions (D) for **Ip_a** of polymeric films prepared through consecutive electropolymerization in individual

phenothiazine solutions. The dashed lines in A and B represent 2 standard errors above and below the estimated smooth function being plotted.

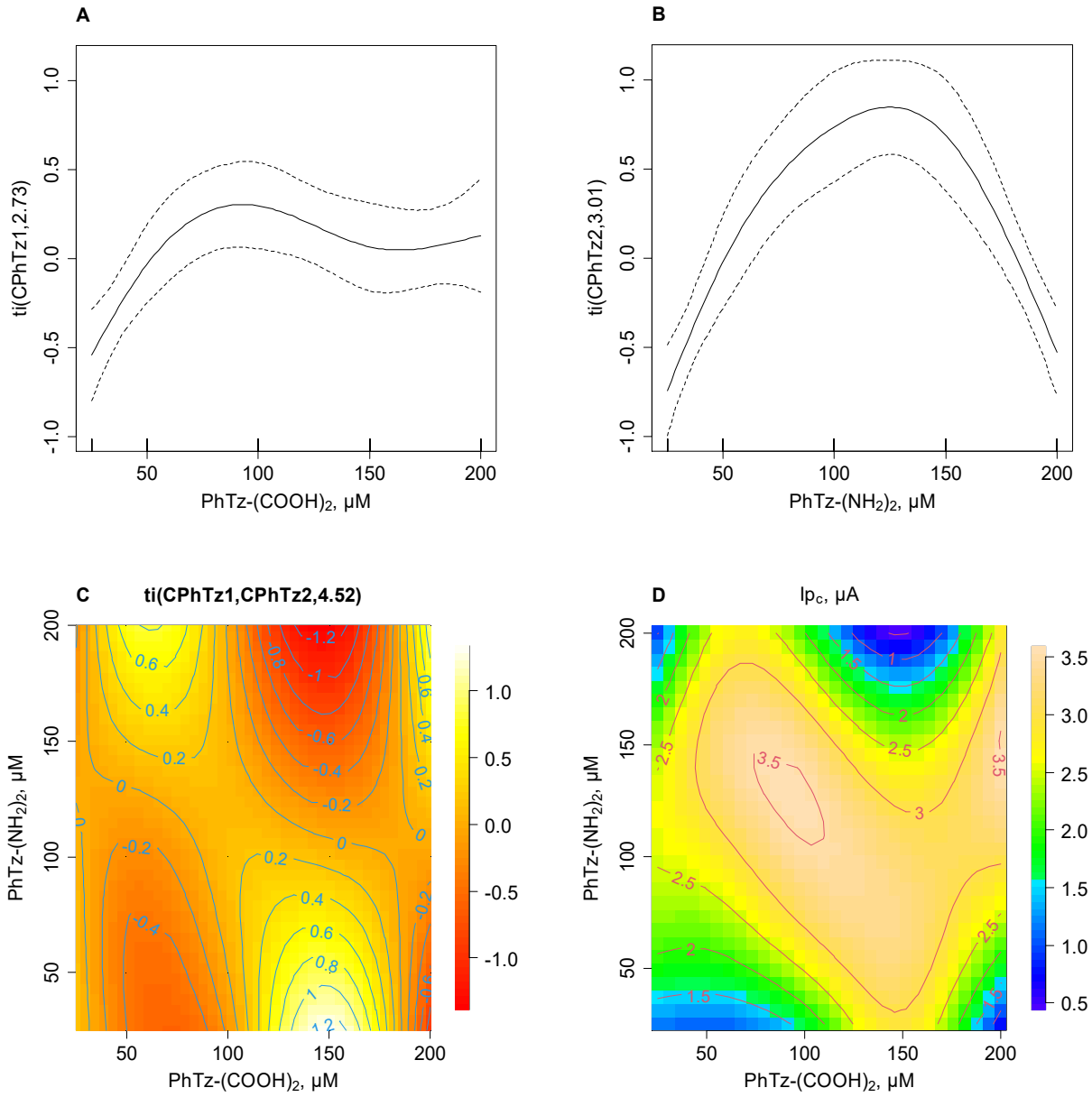

Figure S10. The component smooth functions (A, B, C) and model predictions (D) for $\mathbf{Ip_c}$ of polymeric films prepared through consecutive electropolymerization in individual phenothiazine solutions. The dashed lines in A and B represent 2 standard errors above and below the estimated smooth function being plotted.

Modelling Ip_a and Ip_c of polymeric films prepared through consecutive electropolymerization in individual phenothiazine solutions and immobilized DNA.

Table S4. EDF and Significance (p-value) of smooth terms for models predicting $\mathbf{Ip_a}$ and $\mathbf{Ip_c}$ of polymeric films prepared through consecutive electropolymerization in individual phenothiazine solutions and immobilized DNA.

Smoothing Term	EDF (p-value)	
	$\mathbf{Ip_a}$	$\mathbf{Ip_c}$
ti(CPhTz1)	1.00 (< 0.001)	1.03 (< 0.001)
ti(CPhTz2)	0.00 (0.29)	3.24 (< 0.001)
ti(CPhTz1, CPhTz2)	2.95 (< 0.001)	2.20 (0.006)
Adjusted R^2	0.362	0.462

All smoothing terms were found to be significant for both $\mathbf{Ip_a}$ and $\mathbf{Ip_c}$, except the smoothing term of CPhTz1 for $\mathbf{Ip_a}$ and therefore it almost shrunk to zero. Plots of the component smooth functions for $\mathbf{Ip_a}$ and $\mathbf{Ip_c}$ are presented in Figures S11 and S12 (panels A, B, C), alongside plots of the model predictions (Figures S11 and S12, panel D).

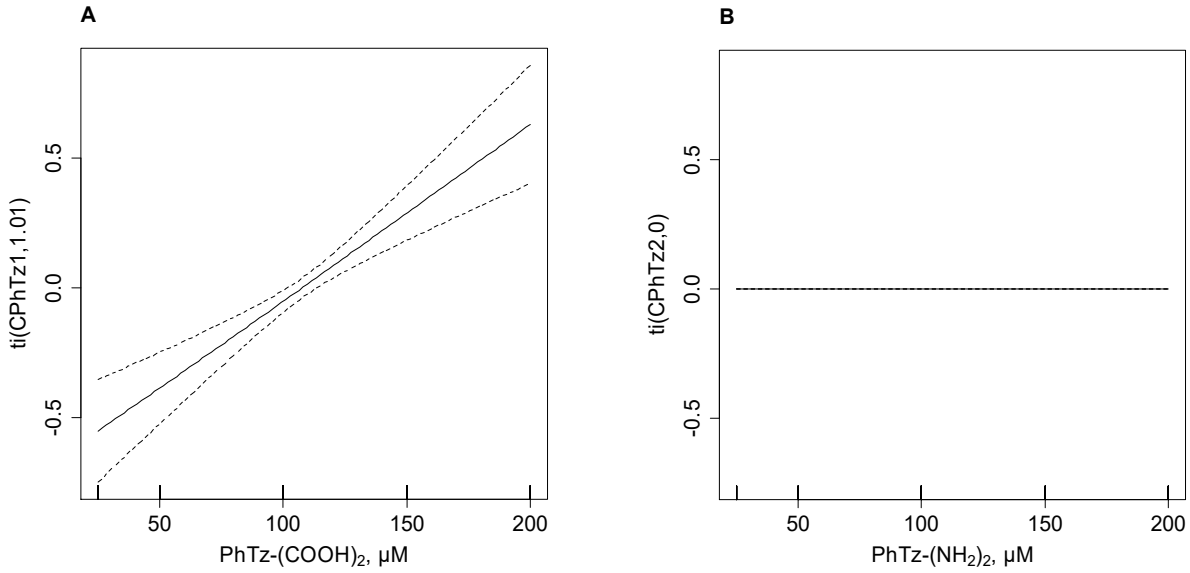

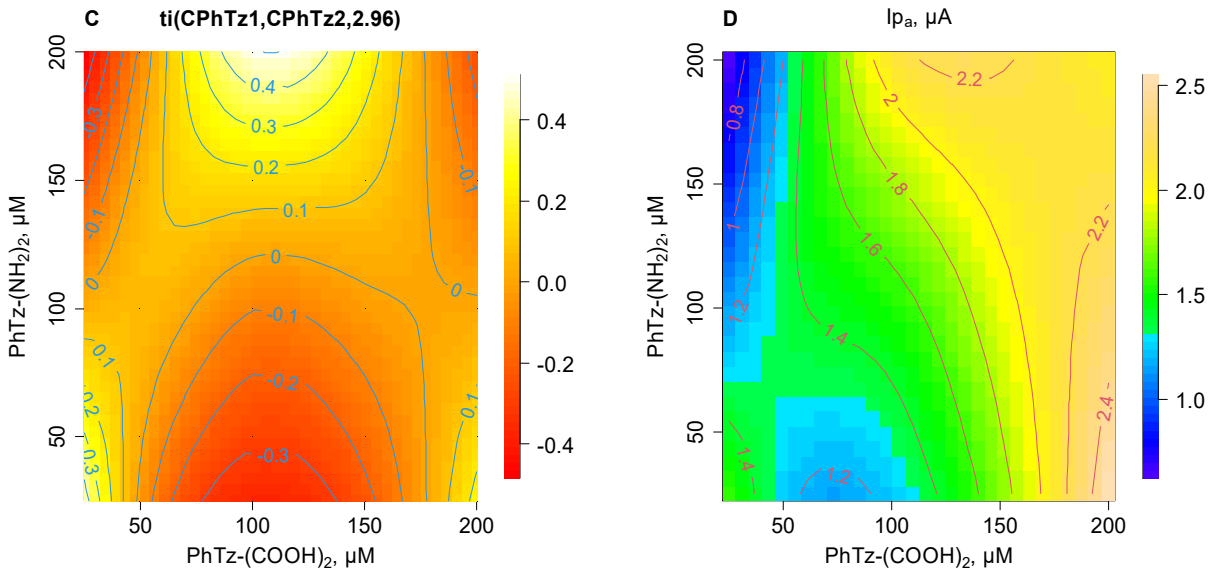

Figure S11. The component smooth functions (A, B, C) and model predictions (D) for **Ip_a** of polymeric films prepared through consecutive electropolymerization in individual phenothiazine solutions and immobilized DNA. The dashed lines in A and B represent 2 standard errors above and below the estimated smooth function being plotted.

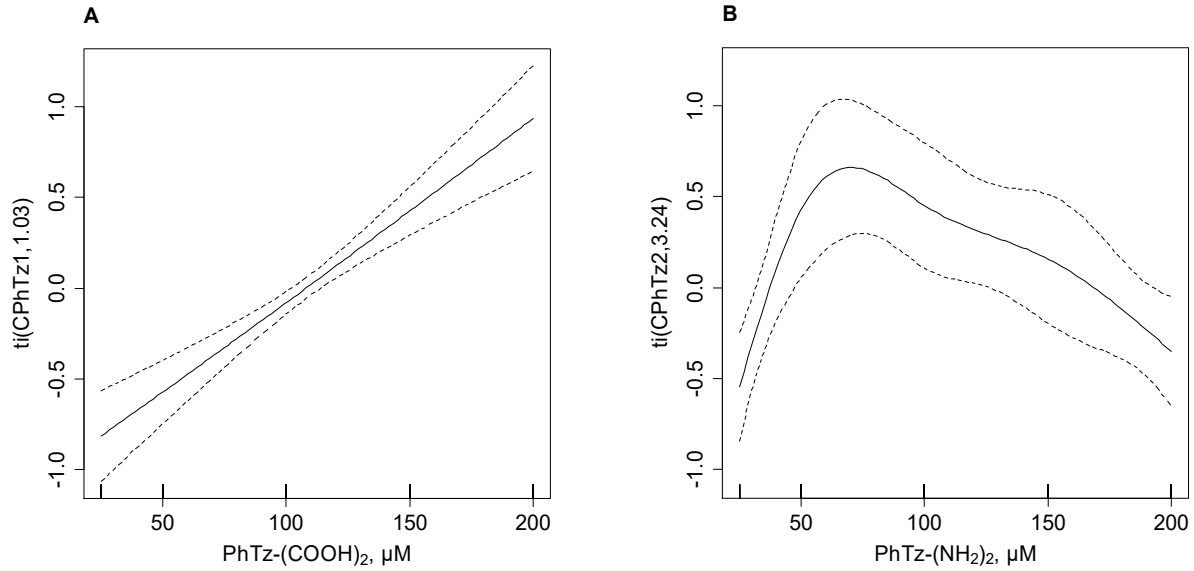

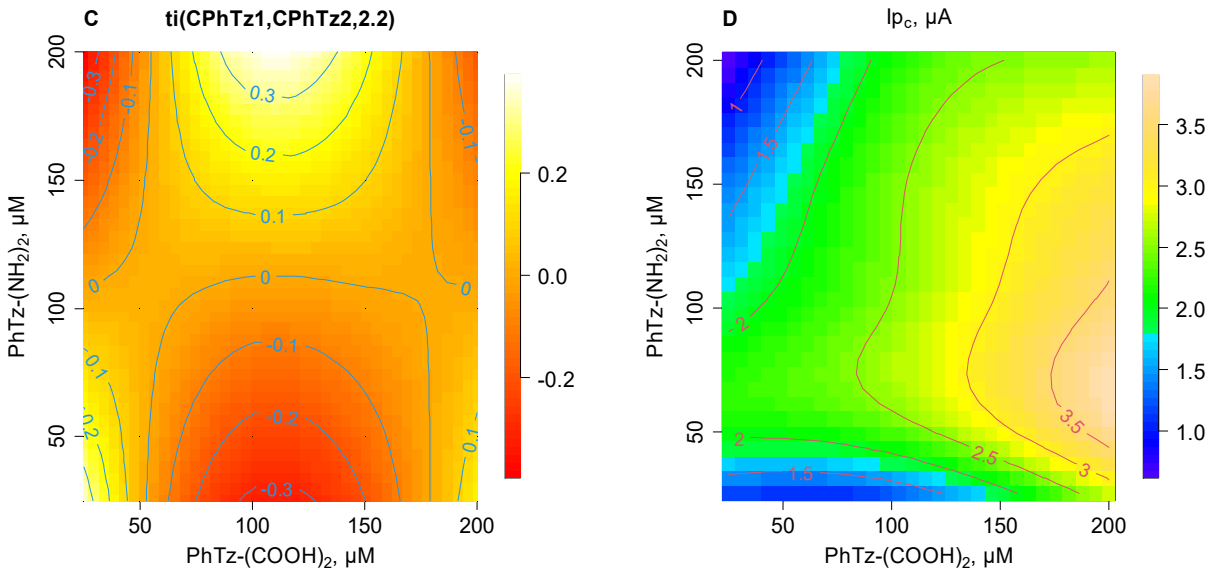

Figure S12. The component smooth functions (A, B, C) and model predictions (D) for **Ip_c** of polymeric films prepared through consecutive electropolymerization in individual phenothiazine solutions and immobilized DNA. The dashed lines in A and B represent 2 standard errors above and below the estimated smooth function being plotted.